IAI Journals.ASM.org

Fibronectin Binding Proteins SpsD and SpsL Both Support Invasion of Canine Epithelial Cells by *Staphylococcus pseudintermedius*

Giampiero Pietrocola,[a] Valentina Gianotti,[a] Amy Richards,[b] Giulia Nobile,[a] Joan A. Geoghegan,[c] Simonetta Rindi,[a] Ian R. Monk,[c] Andrea S. Bordt,[d] Timothy J. Foster,[c] J. Ross Fitzgerald,[b] Pietro Speziale[a]

Department of Molecular Medicine, Unit of Biochemistry, Pavia, Italy[a]; The Roslin Institute and Edinburgh Infectious Diseases, University of Edinburgh, Easter Bush, Midlothian, Scotland, United Kingdom[b]; Department of Microbiology, Moyne Institute of Preventive Medicine, Trinity College Dublin, Dublin, Ireland[c]; Center for Infectious and Inflammatory Diseases, Texas A&M Health Science Center, Houston, Texas, USA[d]

In this study, we investigated the cell wall-anchored fibronectin-binding proteins SpsD and SpsL from the canine commensal and pathogen *Staphylococcus pseudintermedius* for their role in promoting bacterial invasion of canine progenitor epidermal keratinocytes (CPEK). Invasion was examined by the gentamicin protection assay and fluorescence microscopy. An Δ*spsD* Δ*spsL* mutant of strain ED99 had a dramatically reduced capacity to invade CPEK monolayers, while no difference in the invasion level was observed with single mutants. *Lactococcus lactis* transformed with plasmids expressing SpsD and SpsL promoted invasion, showing that both proteins are important. Soluble fibronectin was required for invasion, and an RGD-containing peptide or antibodies recognizing the integrin $\alpha_5\beta_1$ markedly reduced invasion, suggesting an important role for the integrin in this process. Src kinase inhibitors effectively blocked internalization, suggesting a functional role for the kinase in invasion. In order to identify the minimal fibronectin-binding region of SpsD and SpsL involved in the internalization process, recombinant fragments of both proteins were produced. The $SpsD_{520-846}$ and $SpsL_{538-823}$ regions harboring the major fibronectin-binding sites inhibited *S. pseudintermedius* internalization. Finally, the effects of staphylococcal invasion on the integrity of different cell lines were examined. Because SpsD and SpsL are critical factors for adhesion and invasion, blocking these processes could provide a strategy for future approaches to treating infections.

The Gram-positive bacterium *Staphylococcus pseudintermedius* is a common commensal of dogs (1, 2). The bacterium is also the most common pathogen associated with canine otitis externa and pyoderma as well as surgical wound infections and urinary tract infections (3). Sporadic cases of human infection have also been reported, including some in individuals exposed to colonized household pets (4–7). Genome sequence analysis (8, 9) indicates that *S. pseudintermedius* could encode many potential virulence factors, including toxins, enzymes, and surface proteins, some of which can promote adhesion of the bacterium to the surface of epithelial cells (10–13) and to components of the extracellular matrix (14, 15).

Two cell wall-anchored surface proteins that are likely to be important in host tissue colonization and pathogenesis are SpsD and SpsL (Fig. 1) (15). The primary translation product of SpsD from strain ED99 has an N-terminal secretory signal sequence and a C-terminal cell wall-anchoring domain (the sorting signal) comprising an LPXTG motif, a hydrophobic transmembrane domain, and a short sequence rich in positively charged residues. Residues at the N terminus of SpsD are 40% identical to the fibrinogen-binding A domain of FnBPB from *Staphylococcus aureus* and are predicted to fold into three subdomains: N1, N2, and N3. This domain is followed by a connecting region, region C, and a repeat region, region R. SpsL includes a signal sequence at the N terminus followed by an A domain with two IgG-like folds (N2 and N3), a domain containing seven tandem repeats with weak homology to the fibronectin binding repeats of FnBPA from *S. aureus*, and a C-terminal sorting signal.

SpsD and SpsL mediate bacterial adherence to fibrinogen (15) and fibronectin (Fn) (15), while SpsD also binds to cytokeratin 10 and elastin (16). The binding site in fibrinogen for SpsD was mapped to residues 395 to 411 in the γ-chain, while a binding site for SpsD in Fn was localized to the N-terminal region. SpsD also binds to glycine- and serine-rich omega loops within the C-terminal tail region of cytokeratin 10 (16).

Another important Sps protein involved in host colonization is SpsO, which has been demonstrated to mediate adherence to *ex vivo* canine keratinocytes (12). However, the host ligand(s) interacting with SpsO remains to be determined (15).

The SpsO protein of *S. pseudintermedius* is also likely to be involved in colonization of the canine host. It promotes adhesion to *ex vivo* canine corneocytes, as does SpsD, although the ligand(s) recognized by SpsO remains to be identified. Invasive bacteria actively induce their own uptake by phagocytosis into normally nonphagocytic cells, where they establish a protected niche within which they can replicate (17). For example, *S. aureus*, usually considered an extracellular pathogen, can invade a variety of nonpro-

Received 25 April 2015 **Returned for modification** 4 June 2015
Accepted 24 July 2015

Accepted manuscript posted online 3 August 2015

Citation Pietrocola G, Gianotti V, Richards A, Nobile G, Geoghegan JA, Rindi S, Monk IR, Bordt AS, Foster TJ, Fitzgerald JR, Speziale P. 2015. Fibronectin binding proteins SpsD and SpsL both support invasion of canine epithelial cells by *Staphylococcus pseudintermedius*. Infect Immun 83:4093–4102. doi:10.1128/IAI.00542-15.

Editor: A. Camilli

Address correspondence to Pietro Speziale, pspeziale@unipv.it.

V.G. and A.R. contributed equally to this work.

Supplemental material for this article may be found at http://dx.doi.org/10.1128/IAI.00542-15.

doi:10.1128/IAI.00542-15

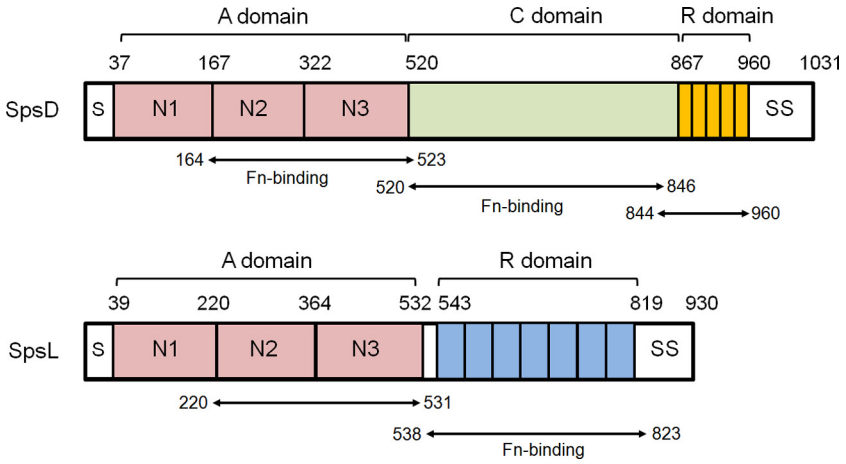

FIG 1 Schematic diagram of SpsD and SpsL proteins from *S. pseudintermedius* ED99. The A domain of SpsD spans residues 37 to 519 following the secretory signal sequence (S), followed by a connecting domain (C; residues 520 to 866) and a repeat region (R). A sorting signal (SS; LPXTG motif, hydrophobic domain, and positively charged residues) occurs at the extreme C terminus. SpsL includes a signal sequence (S) at the N terminus, followed by an A domain (residues 39 to 531), a domain containing seven tandem repeats (R; residues 543 to 818), and a C-terminal sorting signal (SS). The A domains of both proteins align with A domains of the MSCRAMM family of *S. aureus* surface proteins, and each comprises three subdomains, N1, N2, and N3, with N2 and N3 being predicted to form IgG-like folds. The A domains of SpsD and SpsL from ED99 have 30% identity and 50% similarity. The recombinant proteins are indicated, along with ability of each truncated form to bind to fibronectin.

fessional phagocytic cells, explaining its capacity to colonize mucosa and its persistence in tissue after bacteremia. The underlying major molecular mechanism of invasion involves the Fn-binding adhesins FnBPA and FnBPB (18, 19). Fn bridging between FnBPs and $\alpha_5\beta_1$ integrins on the host cell surface is sufficient to induce zipper-type uptake of staphylococci (18–20). The ternary complex promotes integrin clustering and a relay of signals that result in cytoskeletal rearrangements. The rearrangements are accompanied by endocytosis of *S. aureus* and internalization (17).

In this study, we wished to investigate whether *S. pseudintermedius* shares with *S. aureus* the ability to invade nonprofessional phagocytic cells and to determine the bacterial and host components that are involved. We reasoned that both SpsD and SpsL could be involved in the internalization of *S. pseudintermedius* by host cells. The objective of this study was to investigate internalization and its mechanistic basis. The analysis of this process will provide insights into the potential of a vaccine comprising components of SpsD and SpsL for the prevention of canine pyoderma.

MATERIALS AND METHODS

Bacterial strains and culture conditions. *S. pseudintermedius* strain ED99 (formerly M732/99) was isolated from a canine bacterial pyoderma case presented to the Dermatology Service of The Hospital for Small Animals, Division of Veterinary Clinical Sciences, The Royal (Dick) School of Veterinary Studies, The University of Edinburgh. *S. pseudintermedius* strains 264, 324, 326, 327, 328, and 329 were isolated from cases of canine pyoderma and were a kind gift from Neil McEwan, University of Liverpool. *S. pseudintermedius* strains 81852, 91180, 253834, 237425, and 235214/1 were isolated from cases of canine pyoderma and were donated from Istituto Zooprofilattico Sperimentale della Lombardia e della Emilia Romagna, Pavia, Italy. The strains were classified as *S. pseudintermedius* using standard phenotypic tests (21). *S. pseudintermedius* ED99 and its mutants were grown in brain heart infusion (BHI) broth (VWR International Srl, Milan, Italy) at 37°C with shaking. Transformants of *Lactococcus lactis* harboring plasmid pOri23, pOri23::*spsD*, or pOri23::*spsL* (15) were grown in M17 medium (Difco, Detroit, MI, USA) supplemented with 10% lactose, 0.5% glucose, and 10 μg ml^{-1} erythromycin at 30°C without shaking. *Escherichia coli* DC10B (22) and TOPP3 (Stratagene, La Jolla, CA) were grown in Luria agar (LA) and Luria broth (LB) (VWR International Srl).

Reagents, proteins, and antibodies. Human fibronectin was purified from plasma by a combination of gelatin- and arginine-Sepharose affinity chromatography. The purity of the protein was assessed by 7.5% SDS-PAGE and Coomassie brilliant blue staining. To exclude the possibility of trace amounts of contaminants, affinity-purified fibronectin was spotted onto nitrocellulose membranes at different concentrations and overlaid with antifibrinogen and antiplasminogen antibodies (23). The N-terminal fragment of Fn (N29), containing the five N-terminal type I modules, and the gelatin-binding domain (GBD), consisting of four type I modules and two type II modules, were isolated as previously reported (24). Unless stated otherwise, all reagents were purchased from Sigma-Aldrich (St. Louis, MO, USA). The anti-human Fn rabbit polyclonal IgG was purchased from Pierce (Rockford, IL, USA). The mouse monoclonal antibody JBS5 against the human integrin $\alpha_5\beta_1$ was purchased from Merck-Millipore (Darmstadt, Germany). The rabbit polyclonal antibody against the α_5 chain of the $\alpha_5\beta_1$ integrin and the mouse monoclonal antibodies BV7 against the human β_1 chain and B212 against the human β_3 chain of the integrin $\alpha_v\beta_3$ were a generous gift from G. Tarone (University of Turin, Italy). Mouse polyclonal antibodies against region A of SpsD and SpsL were prepared as previously reported (16).

DNA manipulation. DNA encoding regions $SpsD_{164-523}$, $SpsD_{520-846}$, $SpsD_{844-960}$, $SpsL_{220-531}$, and $SpsL_{538-823}$ were amplified by PCR using *S. pseudintermedius* ED99 genomic DNA as the template. Oligonucleotides were purchased from Integrated DNA Technologies (Leuven, Belgium) (see Table S1 in the supplemental material). Restriction enzyme cleavage sites (see Table S1) were incorporated at the 5′ ends of the primers to facilitate cloning into plasmid pQE30 (Qiagen, Chatsworth, CA, USA). Restriction enzymes were purchased from New England BioLabs (Hertfordshire, United Kingdom). The integrity of cloned DNA was confirmed by sequencing (Primmbiotech, Milan, Italy).

Expression and purification of recombinant proteins. Recombinant proteins were expressed from pQE30 in *E. coli* TOPP3 (Stratagene). Overnight starter cultures were diluted 1:50 in LB containing ampicillin (100 μg ml^{-1}) and incubated with shaking until the culture reached an optical density at 600 nm (OD_{600}) of 0.4 to 0.6. Recombinant protein expression was induced by addition of isopropyl 1-thio-β-D-galactopyranoside (0.5 mM) and continued for 2 h. Bacterial cells were harvested by centrifuga-

TABLE 1 Plasmids used for the construction of *spsD*- and *spsL*-null mutants

Plasmid	Description	Reference
pIMAY	Thermosensitive plasmid for allelic exchange	21
pIMAY Δ*spsD*	pIMAY with fragments flanking *spsD*	This paper
pIMAY-Z	pIMAY derivative with a constitutive *lacZ* marker	25
pIMAY-Z Δ*spsL*	pIMAY-Z with fragments flanking *spsL*	This paper

tion and frozen at −80°C. Recombinant proteins were purified from cell lysates by Ni^{2+} affinity chromatography on a HiTrap chelating column (GE Healthcare, Buckinghamshire, United Kingdom). Protein purity was assessed to be 98% by SDS-PAGE, Coomassie brilliant blue staining, and densitometric analysis.

ELISA-type solid-phase binding assays. The ability of immobilized recombinant proteins to interact with soluble human Fn was determined using enzyme-linked immunosorbent assays (ELISAs). Microtiter wells were coated overnight at 4°C with 100 μl of 10 μg ml^{-1} of bacterial protein in 50 mM sodium carbonate, pH 9.5. To block additional protein-binding sites, the wells were treated for 1 h at 22°C with 200 μl of 2% bovine serum albumin (BSA) in phosphate-buffered saline (PBS). The plates were then incubated for 1 h with increasing amounts of Fn. One microgram of the specific anti-Fn rabbit IgG (1:2,000) in PBS with 0.1% BSA was added to the wells, followed by incubation for 90 min. After washing, the plates were incubated for 1 h with peroxidase-conjugated secondary anti-rabbit IgG diluted 1:1,000. After washing, *o*-phenylenediamine dihydrochloride was added and the absorbance at 490 nm was determined. To calculate the relative affinity association constant (K_A) values of each bacterial protein for Fn the following equation was employed: $A = A_{max}[L]K_A/(1 + K_A[L])$, where [L] is the molar concentration of ligand. The dissociation constants (K_D values) were calculated as reciprocals of the K_A values. The assays were performed at least 3 times for each protein.

Construction of *spsD*- and *spsL*-null mutants. Allele replacement mutagenesis of *spsD* and *spsL* was performed using the thermosensitive plasmids pIMAY and pIMAY-Z (Table 1). For generation of the *spsD*-null mutation, approximately 500-bp fragments of DNA flanking the gene were PCR amplified using the AB and CD primers, spliced together, and cloned into the blunt-end ligation pSC-B vector (StrataClone, Agilent Technologies, Santa Clara, CA) before subcloning into pIMAY to produce the pIMAY Δ*spsD* construct. The plasmid was transformed into *E. coli* DC10B before being electrotransformed into *S. pseudintermedius* ED99 at 28°C with selection on 10 μg ml^{-1} chloramphenicol, as previously described for *S. aureus* (25). For generation of the *spsL*-null mutation, a sequence ligase-independent cloning (SLIC) protocol was performed (26) using pIMAY-Z, a derivative of pIMAY with a constitutive *lacZ* marker, to construct pIMAY-Z Δ*spsL*. Once the plasmids were transformed into ED99 at 28°C, growth at the restrictive temperature of 37°C selected for integrants. OUT primers, located outside the flanking regions and gene of interest, were used to determine if integration had occurred upstream or downstream of the chromosomal gene (22). A single colony from each site of integration was inoculated into broth and grown at 28°C and then diluted and grown at 37°C. The *S. aureus* antisense *secY* mechanism within pIMAY (27) was nonfunctional in *S. pseudintermedius*, and the *lacZ* marker was ineffective because plasmid-free cells expressed endogenous β-galactosidase activity. Allele exchange was confirmed by using OUT primer PCR and sequencing the resultant fragment (see Table S2 in the supplemental material).

Release of surface proteins from *S. pseudintermedius* and *L. lactis*. *S. pseudintermedius* and *L. lactis* cells were grown to an OD_{600} of 0.4 to 0.6. Cells were harvested by centrifugation at 7,000 × *g* at 4°C for 15 min, washed 3 times with PBS, and resuspended at an OD_{600} of 40 in lysis buffer (50 mM Tris-HCl, 20 mM $MgCl_2$ [pH 7.5]) supplemented with 30% raffinose. Cell wall proteins were solubilized from *S. pseudintermedius* by incubation with lysostaphin (200 μg ml^{-1}) and from *L. lactis* with mutanolysin (1,000 U/ml) and lysozyme (900 μg ml^{-1}) at 37°C for 20 min in the presence of protease inhibitors (Complete Mini; Roche Molecular Biochemicals, Indianapolis, IN, USA). Protoplasts were recovered by centrifugation at 6,000 × *g* for 20 min, and the supernatants were taken as the wall fractions. The material obtained from *S. pseudintermedius* ED99 and its mutants was adsorbed on IgG-Sepharose columns before Western immunoblotting analysis to remove IgG-binding proteins that would otherwise interfere with the specific antibody staining.

SDS-PAGE and Western immunoblotting. Samples for analysis by SDS-PAGE were boiled for 5 min in sample buffer (0.125 M Tris-HCl, 4% [wt/vol] SDS, 20% [vol/vol] glycerol, 10% [vol/vol] β-mercaptoethanol, 0.002% [wt/vol] bromophenol blue) and separated on 10% (wt/vol) polyacrylamide gels. The gels were stained with Coomassie brilliant blue (Bio-Rad, Hercules, CA, USA). For Western immunoblotting, material was subjected to SDS-PAGE and then electroblotted onto a nitrocellulose membrane (GE Healthcare). The membrane was blocked overnight at 4°C with 5% (wt/vol) skim milk in PBS, washed, and incubated with mouse polyclonal antibody against region A of SpsD or SpsL (1 μg ml^{-1}) for 1 h at 22°C. Following additional washings with 0.5% (vol/vol) Tween 20 in PBS (PBST), the membrane was incubated for 1 h with horseradish peroxidase-conjugated rabbit anti-mouse IgG. Finally, blots were developed using the ECL Advance Western blotting detection kit (GE Healthcare) and an ImageQuantTM LAS 4000 mini-biomolecular imager (GE Healthcare).

Mammalian cell lines and culture conditions. Canine progenitor epidermal keratinocytes (CPEK) were cultured in CnT-0.9 medium (CELLnTEC, Bern, Switzerland), without antibiotics at 37°C in 5% CO_2. The spontaneously immortalized keratinocytes (HaCaT) and the human epithelial cell line HEp-2 were cultured in high-glucose Dulbecco's modified Eagle's medium (DMEM) (Gibco BRL, Rockville, MD, USA) supplemented with 10% heat-inactivated fetal bovine serum (FBS) (EuroClone, Milan, Italy), 2% penicillin and streptomycin, 2% sodium pyruvate, and 2% L-glutamine at 37°C in 5% CO_2. Cells were cultured in T75 flasks to approximately 95% confluence, liberated with trypsin-EDTA (EuroClone), resuspended in invasion medium (growth medium without antibiotics), and plated as reported below for the cell invasion assay.

Cell invasion assay. Cell invasion assays were performed essentially as described previously (28). Briefly, cells were plated at 5 × 10^5 (in 0.4 ml invasion medium) into 24-well plates (Corning) and allowed to attach for 24 h at 37°C. Staphylococcal cultures were grown overnight in BHI at 37°C with shaking. *L. lactis* was grown overnight in M17 broth at 30°C without shaking. The following day, cultures were diluted 1:40 in fresh BHI or M17 medium, respectively, grown to an OD_{600} of 0.4, washed 3 times in PBS, and diluted to obtain 10^7 cells/ml in CnT-BM.2 medium supplemented with 10% FBS plus 2 mM L-glutamine. Bacterial suspensions (1 ml) were added to each well and the plates incubated for 2 h at 37°C. Monolayers were then washed 3 times in PBS to remove unattached bacteria. Medium containing antibiotics (200 μg ml^{-1} gentamicin plus 2% penicillin and streptomycin) was added, and the plate was incubated for an additional 2 h to kill extracellular bacteria. The wells were washed again, and internalized bacteria were released by incubating with 200 μl of H_2O containing 0.1% (vol/vol) Triton X-100. Serial dilutions of the cell lysates were plated in duplicate on BHI agar, and CFU were counted after incubation. All assays were carried out in triplicate. Samples of monolayers were lysed prior to inoculation and plated on BHI agar, and the absence of staphylococcal colonies was noted.

Inhibition of invasion. The Src-family kinase inhibitors PP2, PP3, and CGP77675 (25 μM) were dissolved in dimethyl sulfoxide (DMSO), added to the cell medium at the appropriate concentrations, and preincubated with monolayers for 1 h at 37°C in 5% CO_2 before addition of bacteria. Likewise, wortmannin (20 nM), genistein (200 μM), and cy-

tochalasin D (50 μM) were dissolved in PBS and incubated with cells for 60 min prior to the addition of bacteria. Gentamicin protection assays were then performed as described above, except that no intermediate washing was carried out. To test cell viability during exposure to the Src inhibitors, the compounds were added to cell monolayers for 3 h at 37°C. Then the cells were gently washed with DMEM, trypsinized, and mixed with an equal volume of trypan blue (0.5% [vol/vol] in PBS) for 5 min. Ten microliters of the mixture was placed on a Neubauer chamber, and stained cells were counted by light microscopy. The percentage of dead cells was calculated by dividing the mean number of dead (stained) cells by the total number of cells in 50 microscopic fields and multiplying the result by 100.

Fluorescence microscopy. Bacteria were grown to an OD_{600} of 0.3 (*S. pseudintermedius*) or 0.4 (*L. lactis*), centrifuged, and resuspended in 100 μl PBS. Then, 0.5 μl 10 mM calcein-AM (Molecular Probes, Eugene, OR, USA) was added and incubated for 1 h at 37°C (*S. pseudintermedius*) or 2 h at 30°C (*L. lactis*). Stained bacteria were washed 3 times with PBS and resuspended in 1 ml PBS. Suspensions (100 μl) were added to CPEK monolayers and incubated for 2 h at 37°C to allow internalization. Cells were washed with PBS, counterstained for 1 to 3 min with ethidium bromide (10 μg ml^{-1}), and washed again. Fluorescence microscopy (Olympus BX51; Olympus, Segrate, Italy) was performed using a green filter, a red filter, and white light. Images were captured with a charge-coupled device (CCD) camera and assembled using Adobe Photoshop Creative Suite 2.

Staining of monolayers. Mammalian cells were stained with Giemsa stain modified solution (Sigma) according to the manufacturer's instructions and observed under a light microscope at a magnification of ×20.

Invasion assays with formaldehyde-fixed staphylococci. To perform invasion assays with killed bacteria, staphylococci were fixed in 0.5% formaldehyde in PBS for 1 h, stained with calcein-AM, and subjected to fluorescence microscopy. Alternatively, to analyze the effect of formaldehyde-fixed staphylococci on cell survival, monolayers were stained with Giemsa and observed as reported above.

MTT assay. The MTT [3-(4,5-dimethyl-2-thiazolyl)-2,5-diphenyl-2H-tetrazolium bromide] tetrazolium reduction assay was performed according to the manufacturer's instructions (Sigma).

Statistical methods. Continuous data were expressed as means and standard deviations. Two-group comparisons were performed by Student's *t* test. One-way analysis of variance, followed by Bonferroni's *post hoc* tests, was exploited for comparison of three or more groups. Analyses were performed using Prism 4.0 (GraphPad). Two-tailed *P* values of 0.001 were considered statistically significant.

RESULTS

SpsD and SpsL binding to fibronectin. To localize the Fn-binding sites in SpsD and SpsL, recombinant domains were obtained following PCR amplification of genomic DNA from strain ED99. The cloned SpsD domains included the minimum fibrinogen-binding region (residues 164 to 523) ($SpsD_{164–523}$), a connecting region (region C, residues 520 to 846) ($SpsD_{520–846}$), and a repeat region (region R, residues 844 to 960) ($SpsD_{844–960}$). Two recombinant SpsL domains were expressed: the N-terminal region encompassing residues 220 to 531 ($SpsL_{220–531}$) and the repetitive domain spanning residues 538 to 823 ($SpsL_{538–823}$). As shown in ELISA-type solid-phase binding assays (Fig. 2), recombinant $SpsD_{520–846}$ and $SpsL_{538–823}$ regions bound Fn dose dependently and saturably, while no binding was exhibited by $SpsL_{220–531}$ or $SpsD_{844–960}$. $SpsD_{520–846}$ and $SpsL_{538–823}$ bound Fn in the low nanomolar range ($SpsD_{520–846}$ $K_D = 1.7 \pm 0.38$, $SpsL_{538–823}$ $K_D = 0.81 \pm 0.02$ nM), while $SpsD_{164–523}$ gave a half-maximal binding of 2.19 ± 0.47 μM (data not shown).

Invasion of mammalian cells by *S. pseudintermedius*. Several *S. pseudintermedius* isolates were found to invade canine keratinocyte-derived CPEK. The magnitude of invasion was very similar to or even higher than that of the archetypal invasive *S. aureus* strain Cowan 1 (Fig. 3). Thus, invasion of CPEK is a general property of *S. pseudintermedius*.

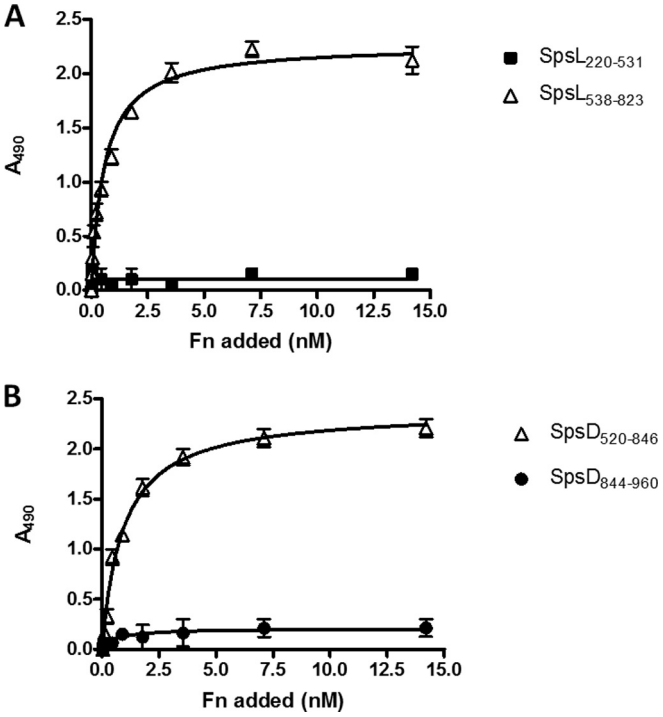

FIG 2 Dose-dependent binding of fibronectin to SpsD and SpsL fragments in an ELISA-type assay. Microtiter wells were coated with $SpsD_{520–846}$, $SpsD_{844–960}$, $SpsL_{220–531}$, and $SpsL_{538–823}$. The wells were probed with increasing amounts of Fn, followed by incubation with rabbit anti-Fn IgG and horseradish peroxidase (HRP)-conjugated goat anti-rabbit IgG. The graph is representative of three experiments, with each point representing the average for triplicate wells.

Requirement for fibronectin for efficient invasion by *S. pseudintermedius* ED99. To investigate the role of soluble plasma-derived Fn in invasion, FBS was passed over a gelatin-Sepharose column to remove soluble Fn before being used in the invasion assay. An 85% reduction in the level of invasion of CPEK was observed when the Fn-depleted FBS was used in the invasion medium compared to unadsorbed FBS. The addition of human Fn to a final concentration of 1 μg ml^{-1} was sufficient to restore the level of invasion to that observed in the presence of whole FBS (Fig. 4A). This suggests that *S. pseudintermedius* strain ED99 can use soluble plasma-derived Fn in the invasion process. Removal of FBS from the assay reduced the invasion level by 95%, suggesting that additional minor components in the FBS other than Fn might contribute. However, although removal of Fn from the gelatin-adsorbed FBS was shown by ELISA and Western blotting, residual internalization can be due to trace amounts of Fn remaining in the invasion medium.

When bacteria were preincubated with increasing amounts of the N29 fragment of Fn and then tested for adherence to or invasion of CPEK, we observed an almost complete inhibition of bacterial internalization. Conversely, no effect was observed when the invasion assay was performed with a high concentration of the GBD of Fn (Fig. 4B). Together, these findings indicate that the N29 domain is specifically involved in adhesion to and invasion of CPEK.

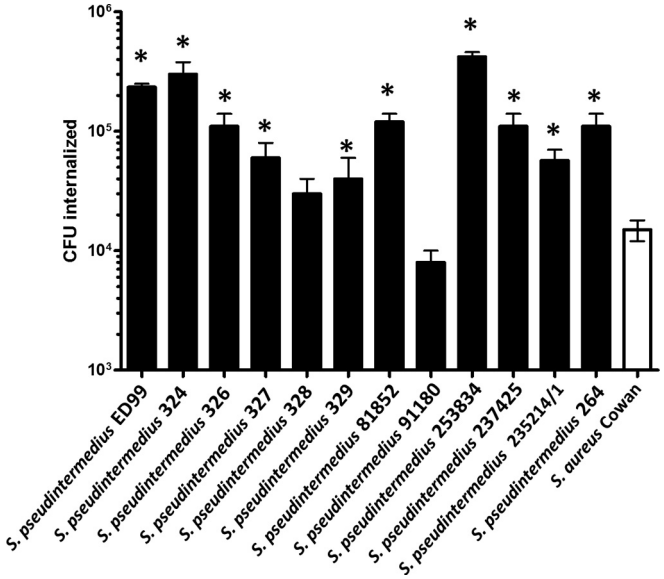

FIG 3 Invasion of CPEK monolayers by *S. pseudintermedius* strains. *S. pseudintermedius* cells were incubated with CPEK monolayers. Extracellular bacteria were killed with gentamicin, and internalized bacteria were quantified by plating lysates on BHI agar. The assay was performed three times. Each point represents the average value for three replicas, and error bars show the standard deviations (SD). Statistically significant ($P < 0.05$; Student's *t* test) differences in values compared with the control value (*S. aureus* Cowan 1) are indicated by an asterisk. The absence of intracellular bacteria in cell cultures was established by lysing samples of the confluent monolayers and plating on BHI agar prior to staphylococcal inoculation.

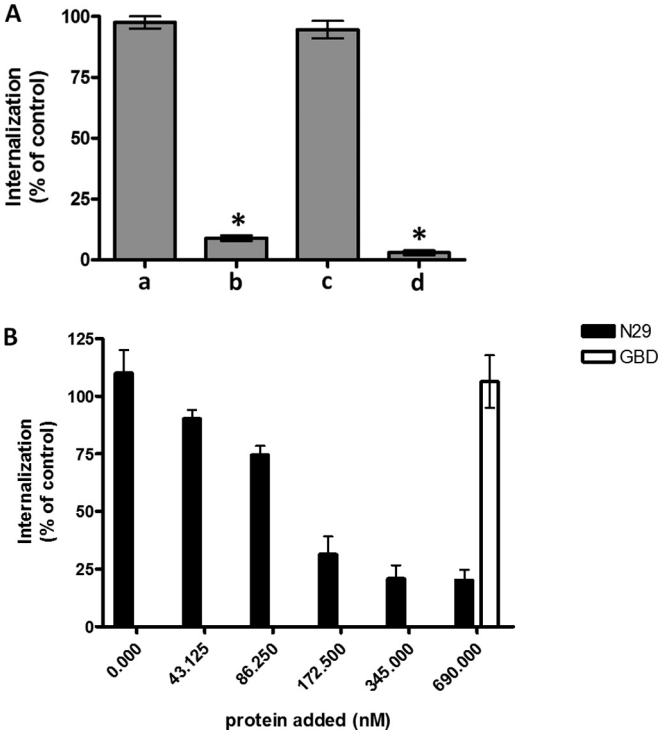

FIG 4 Role of soluble fibronectin on invasion by *S. pseudintermedius*. (A) To evaluate the effect of endogenous fibronectin, the invasion assay was performed in the presence of 10% FBS (a), 10% Fn-depleted FBS (b), and 10% Fn-depleted FBS plus 1 μg/ml soluble human plasma Fn (c) and in the absence of FBS (d). Bacteria were incubated with CPEK monolayers, and internalized bacteria were quantified as described in the legend to Fig. 3. Invasion is expressed as a percentage of that observed in the presence of 10% whole FBS (control; 2×10^5 CFU). Each point represents the average value for three replicates, and error bars represent SD from three independent experiments performed in triplicate. Statistically significant ($P < 0.01$; Student's *t* test) differences in values compared with control value in the presence of FBS are indicated by an asterisk. (B) To determine the effect of the N29 fragment, staphylococci were incubated with increasing concentrations of N29 or 650 nM GBD for 30 min at 22°C. Bacteria were then added to CPEK monolayers and incubated at 37°C for 2 h, and internalized bacteria were quantified as described in the legend to Fig. 3. Invasion is expressed as a percentage of that observed in the absence of inhibitors (control; 2.5×10^5 CFU). Values and error bars represent means and SD from three independent experiments performed in triplicate.

Invasion of CPEK by ED99 mutants and *L. lactis* expressing SpsD or SpsL. Mutants of *S. pseudintermedius* ED99 deficient in SpsD and SpsL were tested for their ability to attach to surface-coating Fn. Mutants defective in either SpsD or SpsL alone adhered as well as the parental strain, while the double mutant defective in both proteins did not bind at all (data not shown). The absence of SpsD or SpsL proteins was confirmed by testing material solubilized from the cell wall with lysostaphin by Western blotting and probing with antibodies against region A of SpsD or SpsL. Both the proteins were absent from the double mutant (Fig. 5A). Conversely, SpsL was expressed normally by the SpsD mutant and *vice versa*.

The SpsD- and SpsL-defective mutants were also tested for invasiveness. Single mutants retained the ability to invade CPEK at the same level as the wild type, while the double mutant lacking both SpsD and SpsL invaded at a much lower level (Fig. 5B).

In order to test whether coreceptors are required for SpsD- or SpsL-mediated invasion, we expressed both *S. pseudintermedius* proteins individually in *Lactococcus lactis* (Fig. 6A). Transformants of *L. lactis* carrying plasmid pOri23::*spsD* and pOri23::*spsL* (Fig. 6A) showed invasiveness similar to that of the wild-type strain ED99 (Fig. 5B), while very low internalization by CPEK was observed with *L. lactis* harboring the empty plasmid (Fig. 6B).

Reduced invasion by the double mutant of ED99 was also assessed by visualizing uptake into CPEK by fluorescent imaging. Bacteria were stained with calcein-AM (green) prior to CPEK invasion, and at the assay endpoint, the fluorescence of external bacteria was visualized with ethidium bromide (red). As shown in Fig. 5C, the wild type and the single mutant strains were observed inside CPEK, while no green fluorescence, indicative of the internalized bacteria, was detected when the double mutant was tested. *L. lactis* expressing SpsL or SpsD behaved similarly (Fig. 6C). Together these results demonstrate that expression of a single adhesin (SpsD or SpsL) is sufficient to confer efficient uptake of bacteria into CPEK.

Localization of Sps domains promoting invasion of CPEK. To identify the domains of SpsD and SpsL that are involved in invasion, recombinant fragments were assessed for inhibition of *S. pseudintermedius* ED99 uptake into CPEK. We found that $SpsD_{520-846}$ (Fig. 7A) and $SpsL_{538-823}$ (Fig. 7B) strongly inhibited internalization, whereas $SpsD_{164-523}$ showed a weak inhibitory effect. The inhibitory effects exhibited by these proteins correlate with their affinities for fibronectin. $SpsL_{220-631}$ and $SpsD_{844-960}$ used at the same concentrations did not interfere with staphylococcal invasion.

Dependence of invasion on integrin $\alpha_5\beta_1$. Immunofluores-

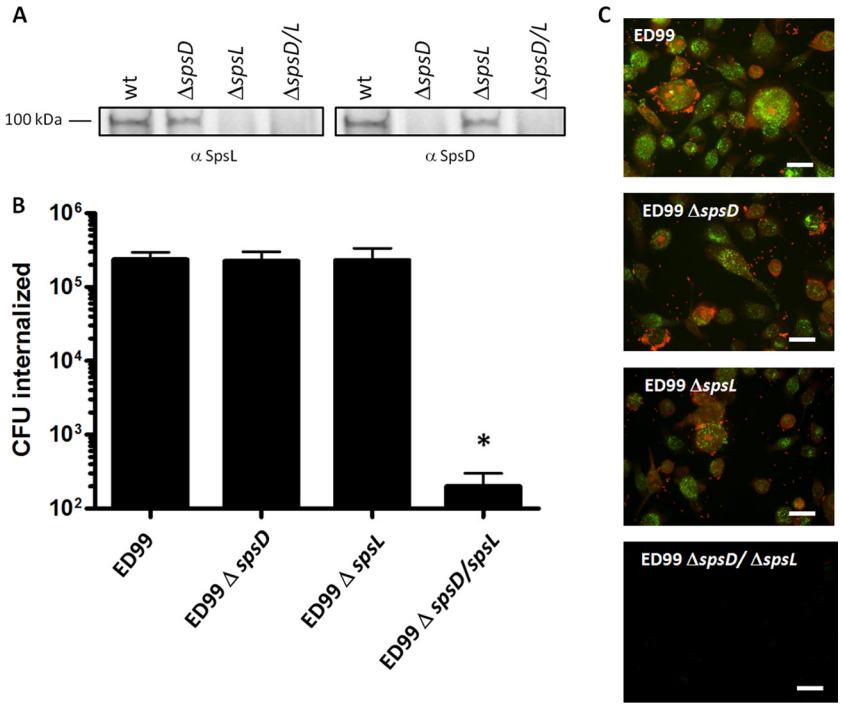

FIG 5 Invasion of CPEK monolayers by *S. pseudintermedius* and its mutants. (A) Expression of SpsD and SpsL proteins. Cell wall proteins from the wild type and mutants were solubilized with lysostaphin, separated by SDS-PAGE and analyzed by Western immunoblotting using mouse anti-SpsD or anti-SpsL and HRP-labeled rabbit anti-mouse IgG. (B) *S. pseudintermedius* wild-type and the Δ*spsD* Δ*spsL* mutant were incubated with CPEK monolayers, and internalized bacteria were quantified as described in the legend to Fig. 3. Bars and error bars show means and SD from three independent determinations performed in triplicate. An asterisk indicates a significant difference ($P < 0.05$; Student's *t* test) compared with the control (invasion with the wild-type strain). (C) Fluorescence microscopy investigating the contribution of SpsD or SpsL to interactions with CPEK. Confluent CPEK monolayers were incubated with calcein-AM-labeled *S. pseudintermedius* to allow internalization, washed with PBS, and counterstained with ethidium bromide. Green fluorescence represents intracellular staphylococci, and red fluorescence represents extracellular bacteria. Bar, 40 μm.

cent antibodies that specifically bind to the α_5 subunit of the human Fn-binding $\alpha_5\beta_1$ integrin stained CPEK, suggesting that the canine cells express an $\alpha_5\beta_1$ integrin that is closely related to the human integrin (Fig. 8A, inset). To test the role of the $\alpha_5\beta_1$ integrin in invasion, CPEK were preincubated with function-blocking anti-$\alpha_5\beta_1$ IgG prior to the addition of *S. pseudintermedius*. Antibodies recognizing the α_5 and the β_1 chains both reduced internalization of *S. pseudintermedius* by more than 80%, whereas antibodies against the β_3 chain of the human $\alpha_v\beta_3$ integrin did not alter invasion (Fig. 8A). This indicates that the $\alpha_5\beta_1$ integrin on canine CPEK is responsible for Fn-mediated bacterial invasion.

Inhibition of invasion by an RGD-containing peptide. The $\alpha_5\beta_1$ integrin recognizes the tripeptide sequence RGD within the cell-binding domain of Fn (29, 30). To investigate the role of this interaction in invasion of *S. pseudintermedius*, the effect of the RGDS peptide was analyzed. Incubation of CPEK with the RGDS peptide reduced the level of invasion by strain ED99 in a dose-dependent manner, while a control peptide RGES had no inhibitory effect (Fig. 8B). This suggests that the interaction of $\alpha_5\beta_1$ with Fn is necessary for efficient invasion of CPEK.

Protein phosphorylation during *S. pseudintermedius* invasion. To identify changes in host cell signaling associated with staphylococcal invasion, the assay was performed in the presence of protein tyrosine phosphorylation inhibitors. Genistein, a tyrosine kinase inhibitor, strongly inhibited internalization, whereas wortmannin, an inhibitor of the phosphatidylinositol-3-phosphate kinase, did not (Fig. 8C). We also tested Src kinase inhibitors and found that both CGP77675 and PP-2 inhibited *S. pseudintermedius* internalization into CPEK. While both inhibitors effectively blocked internalization, CGP77675 appeared to be a more potent inhibitor than PP-2. PP-3, a compound similar to PP-2 but with no significant Src inhibitory activity, had no effect on internalization (Fig. 8C). At the concentrations used, the inhibitors did not affect bacterial adhesion to the CPEK or cause loss of viability, as shown by trypan blue staining (data not shown). To investigate a possible role for actin cytoskeleton rearrangements in *S. pseudintermedius* invasion, we tested cytochalasin D, which interferes with F-actin polymerization. Pretreatment of CPEK with 1 μg/ml cytochalasin D almost completely abolished invasion, demonstrating the involvement of actin cytoskeletal rearrangements (Fig. 8C).

Invasion of Hep-2 and HaCaT cell lines by *S. pseudintermedius*. Human-derived Hep-2 and HaCaT cells were efficiently invaded by *S. pseudintermedius*, and invasion was dependent on Sps proteins. In addition, as reported for CPEK, internalization required the presence of Fn and involved the $\alpha_5\beta_1$ integrin (see Fig. S1 and S2 in the supplemental material).

Alterations to cell monolayers following internalization by *S. pseudintermedius*. To investigate alterations to CPEK, Hep-2, and HaCaT cells following *S. pseudintermedius* invasion, cell monolayers were infected with *S. pseudintermedius* strain ED99 for 2 h prior to gentamicin treatment. Then the cells were incubated for 4 h and 36 h, fixed, and analyzed for morphological changes by light microscopy. A remarkable difference in mor-

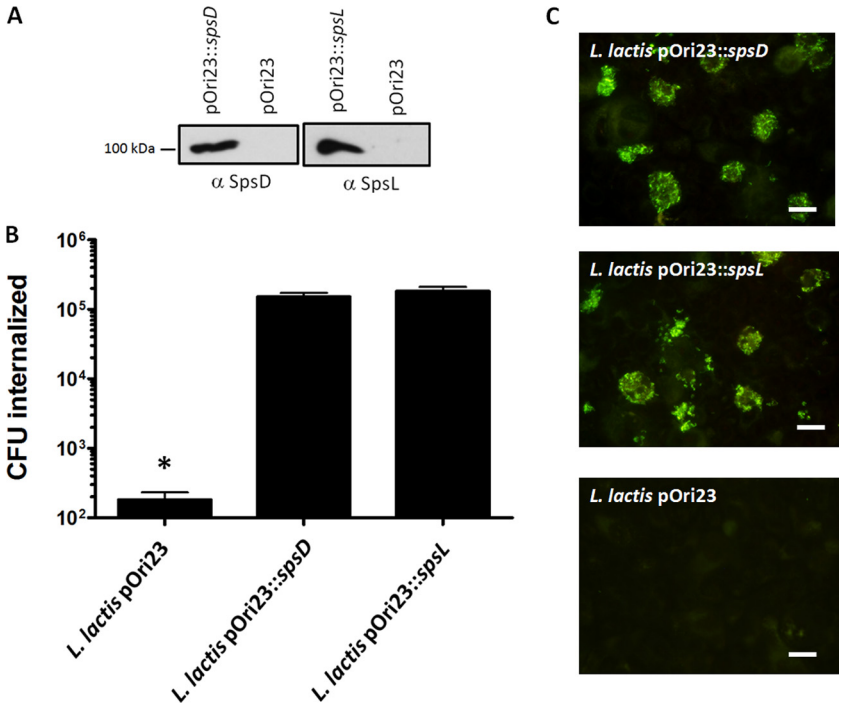

FIG 6 Invasion of CPEK monolayers by *L. lactis*. (A) Expression of SpsD and SpsL by *L. lactis*. Cell wall proteins were solubilized with mutanolysin and lysostaphin, separated by SDS-PAGE, and analyzed by Western immunoblotting using mouse anti-SpsD or anti-SpsL as the primary antibody and HRP-labeled rabbit anti-mouse IgG. (B) CPEK invasion by *L. lactis* expressing SpsD or SpsL. *L. lactis* were incubated with CPEK monolayers, and internalized bacteria were measured as indicated above. Error bars show SD of the means from three independent determinations performed in triplicate. An asterisk indicates a significant difference ($P < 0.05$; Student's *t* test) compared with *L. lactis* pOri23::*spsD* or pOri23::*spsL*. (C) Fluorescent imaging investigating the contribution of SpsD or SpsL to interactions with CPEK monolayers. Confluent CPEK monolayers were incubated with calcein-AM-labeled *L. lactis* to allow internalization. Fluorescence was visualized as in Fig. 5. Bar, 40 μm.

phology was observed between infected and uninfected cell monolayers. Internalization of bacteria by CPEK caused cell detachment and a reduction of the cell density (Fig. 9A). Incubation of Hep-2 cells with strain ED99 for 36 h resulted in rounding and detachment of the cells (see Fig. S3A in the supplemental material). In contrast, HaCaT cells showed a pattern similar to that exhibited by uninfected cells (see Fig. S3C).

The assessment of the cell growth and survival of infected cells by the MTT assay showed that staphylococcal invasion substantially reduced the viability of CPEK (Fig. 9B) and Hep-2 (see Fig. S3B in the supplemental material) cells, whereas HaCaT cells survived to a level comparable to that of the uninfected cells (see Fig. S3D). To further investigate the contribution of bacterial invasion to cell damage, all the cell lines were incubated with the Δ*spsD* Δ*spsL* mutant. Both morphological observations and MTT assays showed that the double mutant did not affect the viability of cells.

DISCUSSION

In this study, we analyzed the molecular mechanism by which *S. pseudintermedius* adheres to and invades canine keratinocytes (CPEK) and the effects of internalization on the viability of the mammalian cells. We found that all strains of *S. pseudintermedius* tested invaded CPEK efficiently. Importantly, we found that both the cell wall-anchored surface proteins SpsD and SpsL efficiently promoted invasion of strain ED99. Single mutants defective in either SpsD or SpsL alone showed no reduction in invasion. Only the double mutant lacking both proteins was defective. Conversely, both SpsD and SpsL promoted efficient uptake of the non-invasive surrogate host *L. lactis* when expressed ectopically from recombinant plasmids. Subdomains within SpsD and SpsL were expressed as recombinant proteins, which allowed identification of regions with a high affinity for Fn and which also strongly inhibited bacterial invasion. Invasion of CPEK was dependent on the presence of Fn, as demonstrated by the markedly reduced uptake upon removal of Fn from the cell culture medium (fetal bovine serum) and the restoration of invasion by supplementation with purified human Fn. We recognize the limitation of using human and bovine Fn to assess the role of this protein in bacterial invasion of a canine cell line. However, it should be noted that there is a high level of similarity between human, bovine, and canine Fn (93 to 94% identity, 98% similarity), so that the use of human or bovine Fn is valid.

In *S. aureus* Fn-binding proteins FnBPA and FnBPB both promote invasion of mammalian cells, where Fn acts as a bridge between the bacterial surface protein which binds to the N-terminal N29 domain by the tandem β zipper mechanism and the $\alpha_5\beta_1$ integrin, which recognizes an RGD motif within C-terminal repeat 10 of Fn (18, 31). The finding that the N-terminal region of Fn and an RGD-containing peptide inhibited *S. pseudintermedius* invasion of CPEK strongly suggests that the same mechanism is employed and involves the Fn binding domains of SpsD and SpsL. Inhibition of invasion of CPEK by monoclonal antibodies recognizing epitopes in the human $\alpha_5\beta_1$ integrin strongly suggests that the canine CPEK express an immuno-cross-reactive integrin that is responsible for bacterial adhesion and invasion.

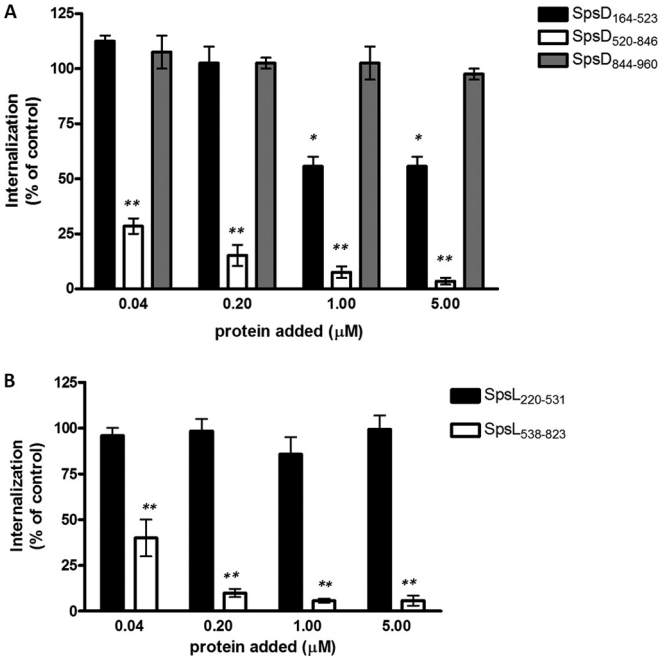

FIG 7 Effect of SpsD and SpsL fragments on invasion of CPEK by *S. pseudintermedius*. CPEK monolayers were incubated with increasing concentrations of $SpsD_{164-523}$, $SpsD_{520-846}$, or $SpsD_{844-960}$ (A) or $SpsL_{220-531}$ or $SpsL_{538-823}$ (B) prior to addition of bacteria. Invasion is expressed as a percentage of that observed in the absence of potential inhibitors (control; 2.2×10^5 CFU). Error bars show SD of the means from three independent determinations performed in triplicate. Statistically significant differences are indicated (Student's two-tailed *t* test; *, $P < 0.05$; **, $P < 0.001$).

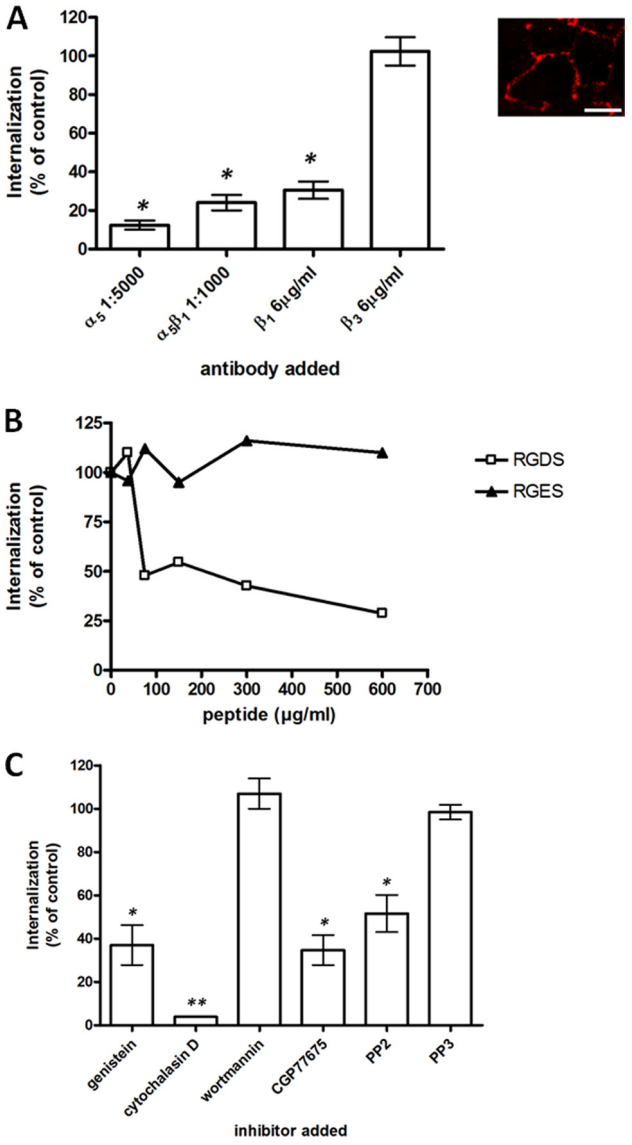

FIG 8 (A) Effect of antiintegrin antibodies on invasion of CPEK by *S. pseudintermedius*. CPEK monolayers were incubated with antibodies against $\alpha_5\beta_1$ and $\alpha_v\beta_3$ integrins prior to the addition of bacteria. After incubation, internalized bacteria were quantified as described above. Invasion is expressed as a percentage of that observed in the absence of antibodies (control; 2.8×10^5 CFU). Bars and error bars represent the means and SD from three independent determinations performed in triplicate. Statistically significant differences are indicated (Student's two-tailed *t* test; *, $P < 0.05$). The inset shows expression of $\alpha_5\beta_1$ integrin by CPEK by staining with immunofluorescent antibodies that specifically bind to the α_5 subunit of the $\alpha_5\beta_1$ integrin. Bar, 40 μm. (B) Effect of an RGD-containing peptide on invasion of CPEK by *S. pseudintermedius*. CPEK were incubated with increasing concentrations of the RGDS or RGES peptide prior to addition of bacteria. After incubation, internalized bacteria were quantified as described above. Invasion is expressed as a percentage of that observed in the absence of peptides (control; 2.3×10^5 CFU). Values are means from three independent determinations performed in triplicate. (C) Effect of kinase inhibitors on invasion of CPEK by *S. pseudintermedius*. CPEK were exposed to genistein, CGP77675, PP2, PP3, wortmannin, and cytochalasin D for 1 h before addition of bacteria. Invasion assays were performed on inhibitor-treated cells three times with similar results. Invasion is expressed as a percentage of that observed in the absence of inhibitors (control; 2.1×10^5 CFU). Bars and error bars represent the means and SD from three independent determinations performed in triplicate. Statistically significant differences are indicated (Student's two-tailed *t* test; *, $P < 0.05$; **, $P < 0.001$).

The Fn bridging mechanism for attachment to and invasion of mammalian cells results from integrin-initiated actin polymerization stimulated by receptor clustering and cell signaling events involving Src (32, 33). Here, invasion of *S. pseudintermedius* was strongly reduced by the Src-specific inhibitors CGP77675 and PP-2, implying that similar mechanisms are responsible. Similar results were obtained when human Hep-2 epithelial cells and HaCaT keratinocytes were tested for invasion by *S. pseudintermedius* ED99. However, certain differences were observed compared to invasion of CPEK. A 10-fold-smaller inoculum was needed for efficient invasion of Hep-2 cells than for HaCaT and CPEK. We speculate that the differences in invasion efficiencies might be due to variations in the density of the $\alpha_5\beta_1$ integrins, although other factors could be involved. Together, these data demonstrate that *S. pseudintermedius* employs a mechanism of host cell invasion similar to that used by *S. aureus* that involves bacterial surface proteins binding to Fn and uptake mediated by integrin $\alpha_5\beta_1$.

Invasion of CPEK and Hep-2 cells resulted in cells detaching and losing viability, whereas HaCaT cells remain unchanged. Thus, in the first two cell lines, invasion by *S. pseudintermedius* triggers a reduction in cell viability. Formaldehyde-killed bacterial cells were actively internalized by the mammalian cells, suggesting that no active expression of invasion-promoting factors was necessary to achieve invasion. Conversely, the lack of effects on host cell survival by killed bacterial cells indicates that additional factors such as secreted toxins are required to induce cell death.

Membrane-damaging toxins that are expressed by intracellular *S. aureus* are major factors in promoting apoptosis (34). *S. pseud-*

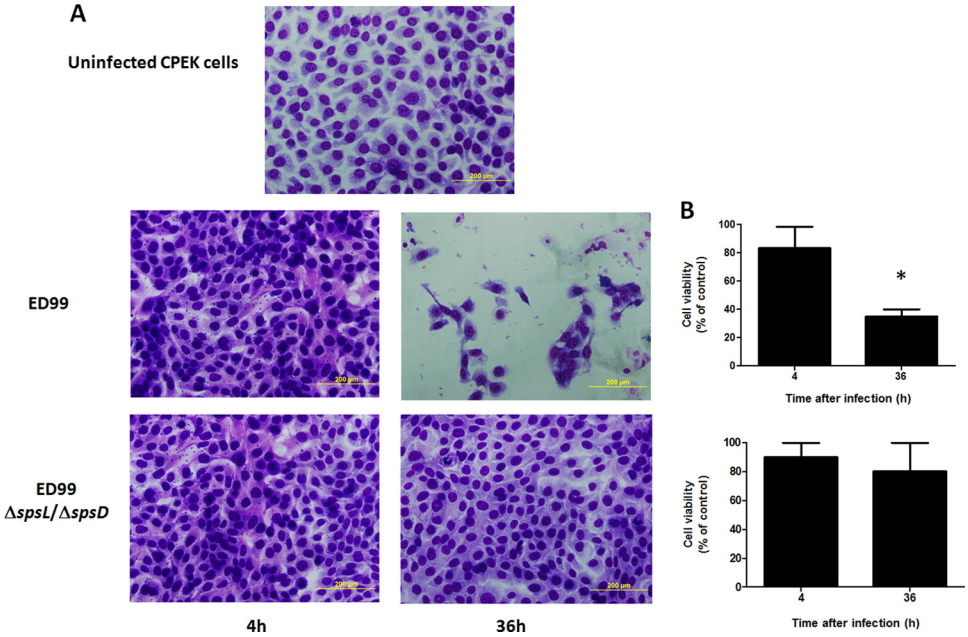

FIG 9 Effects on CPEK following invasion. (A) Alterations to CPEK monolayers after infection with *S. pseudintermedius* and the Δ*spsD* Δ*spsL* mutant. Monolayers were infected with *S. pseudintermedius* prior to gentamicin treatment. Then, the cells were incubated for 4 h and 36 h, stained with Giemsa, and observed for morphological changes by light microscopy. Bars, 200 μm. (B) Assessment of survival of infected cells. Confluent CPEK were infected for 2 h with *S. pseudintermedius* ED99 or the Δ*spsD* Δ*spsL* mutant and then examined at 4 h and 36 h after infection for viability by the MTT assay. Viability was assessed as the percentage of absorbance at 575 nm of treated cells relative to that of solvent-treated controls. Bars and error bars represent the means and SD from three independent determinations performed in triplicate. Statistically significant differences are indicated (Student's two-tailed *t* test; *, $P < 0.05$).

intermedius has the potential to express a bicomponent leukotoxin, Luk-I, which is similar to the Panton-Valentine leucocidin (PVL) of *S. aureus* (35), as well as a homologue of β-toxin and a putative hemolysin (hemolysin III) (8). It can be hypothesized that at least one of these factors is responsible for inducing cell death in CPEK. Indeed, PVL facilitates escape of *S. aureus* from human keratinocyte endosomes and induces apoptosis (34), which might indicate a role here for Luk-I. Studies with mutants lacking one or more of the toxins will help clarify this point.

The initiation of the skin infection canine pyoderma is probably related to the ability of *S. pseudintermedius* to adhere to corneocytes on the surface of the stratum corneum as well as to invade the underlying keratinocytes. *S. pseudintermedius* adheres more strongly to corneocytes from regions of inflamed skin of dogs with atopic dermatitis than to noninflamed areas, suggesting that ligands for bacterial surface protein adhesins are present at higher levels (36). Both SpsD and SpsO mediate bacterial adherence to canine corneocytes, but the host ligands involved are not known (12). In addition, fibronectin is present in the stratum corneum of atopic human skin, where it could provide an abundant ligand, whereas it was not detected in healthy skin (37). Thus, Fn could promote colonization of the stratum corneum as well as invasion of keratinocytes.

In conclusion, we have identified and characterized two fibronectin-binding proteins of *S. pseudintermedius* which are required for adhesion to and invasion of keratinocytes. An appropriate animal model will be required to assess the significance of SpsD and SpsL in the pathogenesis of canine pyoderma and to establish whether these antigens are suitable candidates for a multicomponent vaccine to combat the disease.

ACKNOWLEDGMENTS

We acknowledge funding from Fondazione CARIPLO (Grant Vaccines 2009-3546) to P.S. J.R.F. received funding from Zoetis and Institute strategic funding from BBSRC.

We thank G. Guidetti of the Dipartimento di Biologia e Biotecnologie L. Spallanzani, University of Pavia, Italy, for assistance and advice with fluorescence microscopy.

REFERENCES

1. **Perreten V, Kadlec K, Schwarz S, Grönlund Andersson U, Finn M, Greko C, Moodley A, Kania SA, Frank LA, Bemis DA, Franco A, Iurescia M, Battisti A, Duim B, Wagenaar JA, van Duijkeren E, Weese JS, Fitzgerald JR, Rossano A, Guardabassi L.** 2010. Clonal spread of methicillin-resistant *Staphylococcus pseudintermedius* in Europe and North America: an international multicentre study. J Antimicrob Chemother **65:**1145–1154. http://dx.doi.org/10.1093/jac/dkq078.
2. **Weese JS, van Duijkeren E.** 2010. Methicillin-resistant Staphylococcus aureus and *Staphylococcus pseudintermedius* in veterinary medicine. Vet Microbiol **140:**418–429. http://dx.doi.org/10.1016/j.vetmic.2009.01.039.
3. **Maluping RP, Paul NC, Moodley A.** 2014. Antimicrobial susceptibility of methicillin-resistant *Staphylococcus pseudintermedius* isolated from veterinary clinical cases in the UK. Br J Biomed Sci **71:**55–57.
4. **Gerstadt K, Daly JS, Mitchell M, Wessolossky M, Cheeseman SH.** 1999. Methicillin-resistant *Staphylococcus intermedius* pneumonia following coronary artery bypass grafting. Clin Infect Dis **29:**218–219. http://dx.doi.org/10.1086/520168.
5. **Campanile F, Bongiorno D, Borbone S, Venditti M, Giannella M, Franchi C, Stefani S.** 2007. Characterization of a variant of the SCCmec element in a bloodstream isolate of *Staphylococcus intermedius*. Microb Drug Resist **13:**7–10. http://dx.doi.org/10.1089/mdr.2006.9991.
6. **Kempker R, Mangalat D, Kongphet-Tran T, Eaton M.** 2009. Beware of the pet dog: a case of *Staphylococcus intermedius* infection. Am J Med Sci **338:**425–427. http://dx.doi.org/10.1097/MAJ.0b013e3181b0baa9.
7. **Stegmann R, Burnens A, Maranta CA, Perreten V.** 2010. Human infection associated with methicillin-resistant *Staphylococcus pseudintermedius*

ST71. J Antimicrob Chemother **65:**2047–2048. http://dx.doi.org/10.1093/jac/dkq241.
8. **Ben Zakour NL, Bannoehr J, van den Broek AH, Thoday KL, Fitzgerald JR.** 2011. Complete genome sequence of the canine pathogen *Staphylococcus pseudintermedius*. J Bacteriol **193:**2363–2364. http://dx.doi.org/10.1128/JB.00137-11.
9. **Tse H, Tsoi HW, Leung SP, Urquhart IJ, Lau SK, Woo PC, Yuen KY.** 2011. Complete genome sequence of the veterinary pathogen *Staphylococcus pseudintermedius* strain HKU10-03, isolated in a case of canine pyoderma. J Bacteriol **193:**1783–1784. http://dx.doi.org/10.1128/JB.00023-11.
10. **McEwan NA.** 2000. Adherence by *Staphylococcus intermedius* to canine keratinocytes in atopic dermatitis. Res Vet Sci **68:**279–283. http://dx.doi.org/10.1053/rvsc.2000.0378.
11. **McEwan NA, Kalna G, Mellor D.** 2005. A comparison of adherence by four strains of *Staphylococcus intermedius* and *Staphylococcus hominis* to canine corneocytes collected from normal dogs and dogs suffering from atopic dermatitis. Res Vet Sci **78:**193–198. http://dx.doi.org/10.1016/j.rvsc.2004.09.002.
12. **Bannoehr J, Brown JK, Shaw DJ, Fitzgerald RJ, van den Broek AH, Thoday KL.** 2012. *Staphylococcus pseudintermedius* surface proteins SpsD and SpsO mediate adherence to *ex vivo* canine corneocytes. Vet Dermatol **23:**119–124, e26. http://dx.doi.org/10.1111/j.1365-3164.2011.01021.x.
13. **Latronico F, Moodley A, Nielsen SS, Guardabassi L.** 2014. Enhanced adherence of methicillin-resistant *Staphylococcus pseudintermedius* sequence type 71 to canine and human corneocytes. Vet Res **45:**70. http://dx.doi.org/10.1186/1297-9716-45-70.
14. **Geoghegan JA, Smith EJ, Speziale P, Foster TJ.** 2009. *Staphylococcus pseudintermedius* expresses surface proteins that closely resemble those from *Staphylococcus aureus*. Vet Microbiol **138:**345–352. http://dx.doi.org/10.1016/j.vetmic.2009.03.030.
15. **Bannoehr J, Ben Zakour NL, Reglinski M, Inglis NF, Prabhakaran S, Fossum E, Smith DG, Wilson GJ, Cartwright RA, Haas J, Hook M, van den Broek AH, Thoday KL, Fitzgerald JR.** 2011. Genomic and surface proteomic analysis of the canine pathogen *Staphylococcus pseudintermedius* reveals proteins that mediate adherence to the extracellular matrix. Infect Immun **79:**3074–3086. http://dx.doi.org/10.1128/IAI.00137-11.
16. **Pietrocola G, Geoghegan JA, Rindi S, Di Poto A, Missineo A, Consalvi V, Foster TJ, Speziale P.** 2013. Molecular characterization of the multiple interactions of SpsD, a surface protein from *Staphylococcus pseudintermedius*, with host extracellular matrix proteins. PLoS One **8:**e66901. http://dx.doi.org/10.1371/journal.pone.0066901.
17. **Fraunholz M, Sinha B.** 2012. Intracellular *Staphylococcus aureus*: live-in and let die. Front Cell Infect Microbiol **2:**43. http://dx.doi.org/10.3389/fcimb.2012.00043.
18. **Sinha B, François PP, Nüsse O, Foti M, Hartford OM, Vaudaux P, Foster TJ, Lew DP, Herrmann M, Krause KH.** 1999. Fibronectin-binding protein acts as *Staphylococcus aureus* invasin via fibronectin bridging to integrin alpha5beta1. Cell Microbiol **1:**101–117. http://dx.doi.org/10.1046/j.1462-5822.1999.00011.x.
19. **Peacock SJ, Foster TJ, Cameron BJ, Berendt AR.** 1999. Bacterial fibronectin-binding proteins and endothelial cell surface fibronectin mediate adherence of *Staphylococcus aureus* to resting human endothelial cells. Microbiology **145:**3477–3486.
20. **Fowler T, Wann ER, Joh D, Johansson S, Foster TJ, Höök M.** 2000. Cellular invasion by *Staphylococcus aureus* involves a fibronectin bridge between the bacterial fibronectin-binding MSCRAMMs and host cell beta1 integrins. Eur J Cell Biol **79:**672–679. http://dx.doi.org/10.1078/0171-9335-00104.
21. **Bannoehr J, Ben Zakour NL, Waller AS, Guardabassi L, Thoday KL, van den Broek AH, Fitzgerald JR.** 2007. Population genetic structure of the *Staphylococcus intermedius* group: insights into agr diversification and the emergence of methicillin-resistant strains. J Bacteriol **189:**8685–8692. http://dx.doi.org/10.1128/JB.01150-07.
22. **Monk IR, Shah IM, Xu M, Tan MW, Foster TJ.** 2012. Transforming the untransformable: application of direct transformation to manipulate genetically *Staphylococcus aureus* and *Staphylococcus epidermidis*. mBio **3**(2): e00277-11. http://dx.doi.org/10.1128/mBio.00277-11.
23. **Speziale P, Visai L, Rindi S, Di Poto A.** 2008. Purification of human plasma fibronectin using immobilized gelatin and Arg affinity chromatography. Nat Protoc **3:**525–533. http://dx.doi.org/10.1038/nprot.2008.12.
24. **Zardi L, Carnemolla B, Balza E, Borsi L, Castellani P, Rocco M, Siri A.** 1985. Elution of fibronectin proteolytic fragments from a hydroxyapatite chromatography column. A simple procedure for the purification of fibronectin domains. Eur J Biochem **146:**571–579.
25. **Monk IR, Tree JJ, Howden BP, Stinear TP, Foster TJ.** 2015. Complete bypass of restriction systems for major *Staphylococcus aureus* lineages. mBio **6**(3):e00308-15. http://dx.doi.org/10.1128/mBio.00308-15.
26. **Li MZ, Elledge SJ.** 2007. Harnessing homologous recombination *in vitro* to generate recombinant DNA via SLIC. Nat Methods **4:**251–256. http://dx.doi.org/10.1038/nmeth1010.
27. **Bae T, Schneewind O.** 2006. Allelic replacement in *Staphylococcus aureus* with inducible counter-selection. Plasmid **55:**58–63. http://dx.doi.org/10.1016/j.plasmid.2005.05.005.
28. **Edwards AM, Massey RC.** 2011. Invasion of human cells by a bacterial pathogen. J Vis Exp **2011**(49):2693. http://dx.doi.org/10.3791/2693.
29. **Akiyama SK, Yamada KM.** 1985. The interaction of plasma fibronectin with fibroblastic cells in suspension. J Biol Chem **260:**4492–4500.
30. **Pytela R, Pierschbacher MD, Ruoslahti E.** 1985. Identification and isolation of a 140 kd cell surface glycoprotein with properties expected of a fibronectin receptor. Cell **40:**191–198. http://dx.doi.org/10.1016/0092-8674(85)90322-8.
31. **Edwards AM, Potter U, Meenan NA, Potts JR, Massey RC.** 2011. *Staphylococcus aureus* keratinocyte invasion is dependent upon multiple high-affinity fibronectin-binding repeats within FnBPA. PLoS One **6:**e18899. http://dx.doi.org/10.1371/journal.pone.0018899.
32. **Agerer F, Michel A, Ohlsen K, Hauck CR.** 2003. Integrin-mediated invasion of *Staphylococcus aureus* into human cells requires Src family protein-tyrosine kinases. J Biol Chem **278:**42524–42531. http://dx.doi.org/10.1074/jbc.M302096200.
33. **Fowler T, Johansson S, Wary KK, Höök M.** 2003. Src kinase has a central role in in vitro cellular internalization of *Staphylococcus aureus*. Cell Microbiol **5:**417–426. http://dx.doi.org/10.1046/j.1462-5822.2003.00290.x.
34. **Chi CY, Lin CC, Liao IC, Yao YC, Shen FC, Liu CC, Lin CF.** 2014. Panton-Valentine leukocidin facilitates the escape of *Staphylococcus aureus* from human keratinocyte endosomes and induces apoptosis. J Infect Dis **209:**224–235. http://dx.doi.org/10.1093/infdis/jit445.
35. **Prevost G, Bouakham T, Piemont Y, Monteil H.** 1996. Characterisation of a synergohymenotropic toxin produced by *Staphylococcus intermedius*. FEBS Lett **381:**272.
36. **McEwan NA, Mellor D, Kalna G.** 2006. Adherence by *Staphylococcus intermedius* to canine corneocytes: a preliminary study comparing noninflamed and inflamed atopic canine skin. Vet Dermatol **17:**151–154. http://dx.doi.org/10.1111/j.1365-3164.2006.00503.x.
37. **Cho SH, Strickland I, Boguniewicz M, Leung DY.** 2001. Fibronectin and fibrinogen contribute to the enhanced binding of *Staphylococcus aureus* to atopic skin. J Allergy Clin Immunol **108:**269–274. http://dx.doi.org/10.1067/mai.2001.117455.